Interactions between hydro-soluble degradation products from a radio-oxidized polyesterurethane and Eu(III) in contexts of repositories for low and intermediate level radioactive waste

Elodie Fromentin, Diane Lebeau, Alexandre Bergounioux, Muriel Ferry, Pascal E. Reiller

Elodie Fromentin, Diane Lebeau, Alexandre Bergounioux, Muriel Ferry and Pascal E. Reiller*

Interactions between hydro-soluble degradation products from a radio-oxidized polyesterurethane and Eu(III) in contexts of repositories for low and intermediate level radioactive waste

https://doi.org/10.1515/ract-2019-3122
Received February 19, 2019; accepted August 28, 2019; published online September 21, 2019

Abstract: The complexation of Eu(III) by hydro-soluble degradation products (HDPs) from a radio-oxidized polyesterurethane is investigated. The polyesterurethane Estane 5703® (PURe) is radio-oxidized at 1000 kGy with γ-rays at room temperature. The polymer is then hydrolysed by a simplified artificial cement pore water solution (pH 13.3) for 31 days at 60 °C. The HDPs within the leachate are characterized using gas chromatography-mass spectrometry, ionic chromatography, and TOC analyser. The complexation of Eu(III) is studied by time-resolved luminescence spectroscopy (TRLS). The main HDPs are adipic acid – hexane-1,6-dioic acid – and butane-1,4-diol. Unlike HDPs from non-irradiated PURe, the HDPs from 1000 kGy γ-irradiated PURe do form complexes with Eu(III) at pH 13.3. Neither adipate nor butane-1,4-diol are responsible for this complexation. The existence of several types of complexes is evidenced by TRLS and electrospray ionization mass spectroscopy (ESI-MS): complexation reactions and operational constants are proposed. The complexes formed at high pH (from 10 to 13) are different from the lower pH complexes. The lower pH complexes are studied by ESI-MS and two ligands are identified: adipate and an oligomer.

Keywords: Europium, polyesterurethane, hydro-soluble degradation products, radio-oxidized polymers, cementitious wastes.

1 Introduction

Knowledge of interactions between radionuclides and organics contaminants from radio-oxidized polymers – generated during exploitation, maintenance, and dismantling of nuclear fuel cycle facilities [1] – is crucial for assessing the mobility of radionuclides near nuclear waste geological disposals [2–6]. Contaminated polymers should be disposed in primary cemented packages and in cemented over-packages in intermediate level long-lived waste (ILW-LL). Deep geological disposals for ILW-LL is considered in France, in the Callovo-Oxfordian clay envisaged as geological barrier [7]. Engineered as well as confinement barriers would be designed in concrete.

After closure of the disposal site, pore water from the host rock will diffuse through the cementitious barriers, becoming alkaline [8], and reach the ILW-LL packages' cores at a time that depends on water permeability of the host rock. At that time, radio-oxidized polymers should be degraded by leaching and alkaline hydrolysis. The resulting products are called hydro-soluble degradation products (HDPs). There is evidence that irradiated polymers induces bacterial nitrate reduction [9], and that HDPs are complexing radionuclides [3–6, 10–13]. Most of the latter studies were focused on complexation by isosaccharinic acid – a glucose isomer and HDP from non-irradiated cellulose [10–13]. Van Loon and Hummel [3] investigated the complexing power of HDPs from two ion-exchange resins. The HDPs from the non-irradiated resins did not complex metals, whereas the HDPs from irradiated resins did. Irradiation seemed to trigger ligands formation [14]. Among HDPs from irradiated resins, oxalate and an unidentified ligand pool were evidenced [3]. Another study of HDPs from a radio-oxidized polyetherurethane shows that ligands were also created by radio-oxidation [4].

Recently, the complexation of lanthanides and actinides by HDPs from γ-irradiated PVC (γ-PVC) was reported [5, 6]. Reiller et al. [5] shown that HDPs from a γ-PVC formed complexes with Eu(III) – analogue of actinides(III) –, which increased $Eu(OH)_3$ solubility from neutral to alkaline pH. Baston et al. [6] shown that HDPs from a γ-PVC, and from γ-irradiated additives, enhanced solubility for Pu and for U(VI). In both studies the ligand pool was occurring via an unidentified ligand pool as for irradiated resins [3].

In this study, we studied a polyesterurethane Estane 5703® (PURe) resin, used in the formulation of gloves for glove boxes in the nuclear industry. Eu(III), chosen to

***Corresponding author: Pascal E. Reiller,** Den – Service d'Etudes Analytiques et de Réactivité des Surfaces (SEARS), CEA, Université Paris-Saclay, F-91191, Gif-sur-Yvette Cedex, France,
E-mail: pascal.reiller@cea.fr
Elodie Fromentin, Diane Lebeau, Alexandre Bergounioux and Muriel Ferry: Den – Service d'Études du Comportement des Radionucléides (SECR), CEA, Université Paris-Saclay, F-91191, Gif-sur-Yvette Cedex, France

investigate the complexing power of HDPs as a non-radioactive chemical analogue of actinides(III) [15], is showing luminescent properties that makes it suitable for both complexation studies and chemical environment probing by Time-Resolved Luminescence Spectroscopy (TRLS) [16–21], including complex organic mixtures [5, 22–26].

As it is necessary to improve the knowledge of chemical structures and functionalities of ligand pools to ascertain the knowledge of the complexing power of HDPs, characterization of the degradation products issued from a γ-irradiated PURe (γ-PURe) were led to identify the main HDPs constituents [27, 28]. Adipic acid – hexane-1,6-dioic acid – was shown to be the main HDP from PURe, and being able to complex Eu(III) under mildly acidic conditions [18, 29]. Considering the source term, adipic acid does not seem to be responsible for the complexation of analogous radionuclides under alkaline conditions [29].

After having quantified the role of adipate ion on the speciation of Eu(III) [29], we will here investigate the real Eu(III)-HDPs system in TRLS and try to identify ligands from the pool in electrospray ionization mass spectrometry. The TRLS spectra and luminescence decay time evolutions of the Eu(III)-HDPs systems will also be discussed giving indications on the ligand (pool) character.

2 Materials and methods

2.1 Production of HDPs

PURe, which three precursors are shown in Fig. S1 of the Supplementary Information (SI), was kindly provided by Lubrizol. The physical properties are described in Fromentin et al. [27]. The critical thickness, which ensure homogeneous radio-oxidation is $L_c = 0.62$ mm – see details in Section S2 of the SI.

As PURe was received as granules, homogeneous radio-oxidation required shaping into films – see details in Section S2 of the SI. Experimental thickness of the obtained films is $L_{exp} = 0.20 \pm 0.04$ mm (average of 200 films). Films were irradiated (IONISOS, France), under air at room temperature, using γ-rays (^{60}Co source) at 0.7 kGy · h^{-1}, in test tubes covered by a beaker to limit dust deposition onto the samples, while allowing air to flow inside the container. Dosimetry was performed using radio-chromic (Red Perspex) dosimeters. No electronic correction was made to account for electronic density difference between water and PURe. After irradiation, the absorbed dose was 10^3 kGy with less than 6 % uncertainty.

Aliquots of 1 g of non-irradiated and γ-PURe were hydrolysed for 31 days at 60 °C under inert atmosphere (N_2) into 10 g of a simplified artificial cement pore water (SACPW) solution [5] – 0.16 mol · kg$_w^{-1}$ KOH (Sigma-Aldrich, 90 %) and 0.07 mol · kg$_w^{-1}$ NaOH – in PFA bottles (Thermo Scientific Nalgene). The pH values were regularly measured using a combined pH-microelectrode and kept constant at 13.3 ± 0.05 by regular weighed addition of a tenfold concentrated SACPW solution to the medium. The 4 points calibrations of the pH-meter were made with 3 commercial buffer solutions (SI Analytics, pH 3.99, 7.01, and 10.06 at 20 °C) and a $Ca(OH)_2$(s) (Acros Organics, 98 %) suspension filtered out just before use (pH 12.6 at 20 °C).

After 31 days the hydrolysed polymer samples were separated from solutions by two filtrations – 0.22 µm PVDF filter on Buchner, plus 0.2 µm PES filter on syringe – in order to preserve the measuring instruments. The final solutions will be noted leachates in the following and contained the HDPs.

The total organic carbon (TOC) released was measured as previously described [28].

Leachates of radio-oxidized polymers can produce coloured solutions. A UV-Visible spectrum of a 150 dilution of the leachate in the SACPW solution was obtained on Shimadzu 2550 spectrophotometer.

Carboxylic acids were quantified by ionic chromatography (ICS-3000, Dionex) – see procedure described in Fromentin et al. [28]. The uncertainty (2σ) was estimated to be 9 %.

BDO was quantified using gas chromatography-mass spectrometry (GC-MS) (Agilent 7890B GC, with a 5977A MSD mass spectrometer, electron-impact ionization mode and quadrupole analyser). The GC system and analysis procedures are detailed in Section S3.1 of the SI.

2.2 Complexation study

The europium(III) stock solution was prepared by dissolving Eu_2O_3 (99.9 %, Alfa Aesar) into 0.1 mol · kg$_w^{-1}$ $HClO_4$ (60 %, Fisher Scientific). Solutions were prepared by diluting leachates into a 0.1 mol · kg$_w^{-1}$ $NaClO_4$ solution and adding an aliquot of the europium(III) stock solution to reach 10^{-6} mol · kg$_w^{-1}$. The pH values were measured just before TRLS measurements.

The solution from Eu_2O_3 dissolution in $HClO_4$ produced a high level of adducts during mass spectrometry analyses; $Eu(NO_3)_3{:}5H_2O$ (≥98.5 %, Fluka) was used instead. A stock solution of 10^{-2} mol · kg$_w^{-1}$ europium was prepared.

The TRLS experimental set-up – pulsed laser, optical parametric oscillator (OPO), type of fluorescence cells,

energy monitoring, and spectrometer –, and determination of luminescence decay times were previously described [29]. The emission signal was collected after a 10 µs delay (D), during a 300 µs gate width (W). Excitation wavelengths, λ_{exc}, are chosen either as the $^7F_0 \rightarrow {}^5L_6$ transition, i. e. 393.8 nm [30], or within the span 390–400 nm. The spectra presented in this work were obtained after 4000 accumulations unless noted otherwise. For each spectrum, the background noise is subtracted and the luminescence is normalized by the average of 100 laser shots energy after the acquisition.

Structural identification of the complexes was done using mass spectrometry (ESI-MS-MS) analyses using a Q-Tof II Micromass (Waters) mass spectrometer equipped with an electrospray ionization (ESI) source and a time-of-flight (TOF) analyser, in positive-ion mode. The capillary and sample cone voltages were set to 3000 and 60 V, respectively. The source and desolvation temperatures were set at 100 and 150 °C, respectively. For MS-MS analyses, the applied collision voltage was between 20 and 40 V. All data analyses were done using MassLynx Software (Waters).

Solutions were prepared by diluting leachates by weighing into milliQ water and an aliquot of the Eu(III) stock solution from $Eu(NO_3)_3{:}5H_2O$ in order to reach 10^{-4} mol·kg$_w^{-1}$. The pH value was measured just before tandem mass spectrometry (ESI-MS-MS) analyses.

Following Fromentin and Reiller [29], speciation calculations were done in the framework of the specific interaction theory (SIT) [31]. The main thermodynamic constants and specific interaction ion parameters are recalled in Tables 1 and 2.

Table 1: Thermodynamic constants for Eu and adipic acid.

Reactions	$Log_{10}K°$ (±1σ)	References
$H_2O \rightleftarrows H^+ + OH^-$	−14.00 ± 0.01	[31]
$Adip^{2-} + H^+ \rightleftarrows AdipH^-$	5.49 ± 0.02	[29]
$AdipH^- + H^+ \rightleftarrows AdipH_2(aq)$	4.48 ± 0.01	[29]
$Eu^{3+} + H_2O \rightleftarrows Eu(OH)^{2+} + H^+$	−7.64 ± 0.04	[32]
$Eu^{3+} + 2H_2O \rightleftarrows Eu(OH)_2^+ + 2H^+$	−15.1 ± 0.2	[32]
$Eu^{3+} + 3H_2O \rightleftarrows Eu(OH)_3 + 3H^+$	−23.7 ± 0.1	[32]
$Eu^{3+} + CO_3^{2-} \rightleftarrows Eu(CO_3)^+$	8.1 ± 0.2	[32]
$Eu^{3+} + 2CO_3^{2-} \rightleftarrows Eu(CO_3)_2^-$	12.1 ± 0.3	[32]
$Eu^{3+} + 2CO_3^{2-} \rightleftarrows Eu(CO_3)_3^{3-}$	13.8 ± 0.3	[33, 34]
$Eu(OH)_3(am) + 3H^+ \rightleftarrows Eu^{3+} + 3H_2O$	−17.6 ± 0.8	[32]
$Eu_2(CO_3)_3(cr) \rightleftarrows 2Eu^{3+} + 3CO_3^{2-}$	−35.0 ± 0.3	[32]
$EuOHCO_3(cr) \rightleftarrows Eu^{3+} + CO_3^{2-} + OH^-$	−21.7 ± 0.1	[32]
$EuOHCO_3(cr) + H^+ \rightleftarrows Eu^{3+} + CO_3^{2-} + H_2O$	−7.7 ± 0.1	[32]
$Eu^{3+} + Adip^{2-} \rightleftarrows EuAdip^+$	3.88 ± 0.40	[29]

3 Results and discussion

3.1 Quantification of HDPs

Figure 1 shows the mass balances on HDPs normalized to one kilogram of non-irradiated PURe and 10^3 kGy γ-PURe. The corresponding carbon concentrations in mol$_C$·kg$_w^{-1}$ are reported in Table S1 of the SI. The mass balance of the non-irradiated material seems complete and the main HDPs are adipic acid and BDO. These two molecules are produced by ester functions hydrolysis of the soft segments (Fig. S1 of the SI). Due to the high uncertainty on BDO quantification, no difference on the mass balances can be evidenced between the non-irradiated PURe and the γ-PURe.

Knowing adipate concentration in HDPs and the Eu(III) complexation constants [29], the Eu(III) speciation in leachates was calculated. Under these conditions, adipate ions should not be able to complex Eu(III) in an alkaline medium (from pH 10). At pH 13.3, which is the pH value of leachates, Eu(III) should predominantly be $Eu(OH)_3(aq)$ and/or $Eu(OH)_3(am)$.

3.2 UV Visible spectrum analysis

The absorption spectrum (Fig. S2 of the SI) shows a wide increasing absorption region from 450 down to 220 nm, with some typical humps in the UV region. Applying a decomposition on the spectrum [35, 36], three Gaussian components at 237, 273, and 317 nm are obtained – uncertainties in Table S2 of the SI, and correlation matrix in Table S3 of the SI. In view of the particularly large width at mid-height of these components, they should reflect the composition of other thicker bands. However, as in the case of natural organic matter, it is impossible to attribute these components to transitions from particular molecules. One can remark that the particularly large third component do not represent the absorption tail above 380 nm. As proposed elsewhere it may be the result of a continuum of coupled states [37] that have not been identified, yet.

3.3 Eu(III) complexation by HDPs

3.3.1 Evidence of complexation phenomenon in alkaline medium

The TRLS spectra of Eu(III) in the SACPW solution is shown in Fig. S3a of the SI. Eu(III) – mostly $Eu(OH)_3(aq)$ see Fig. S4 of the SI –, is non-luminescent under these

Table 2: Specific ion interaction coefficients used in this study.

Ion interaction coefficient	Value (±1σ)	References
$\varepsilon(H^+, ClO_4^-)$	0.14 ± 0.02	[31]
$\varepsilon(Na^+, OH^-)$	0.04 ± 0.01	[31]
$\varepsilon(Na^+, CO_3^{2-})$	−0.08 ± 0.03	[31]
$\varepsilon(Na^+, Adip^{2-})$	0.215 ± 0.006	[29]
$\varepsilon(Na^+, AdipH^-)$	0.135 ± 0.006	[29]
$\varepsilon(AdipH_2(aq), NaClO_4)$	0.037 ± 0.009	[29]
$\varepsilon(AdipH_2(aq), NaCl)$	0.105 ± 0.005	[29]
$\varepsilon(Eu^{3+}, ClO_4^-)$	0.49 ± 0.03	Analogy with Am^{3+} [31]
$\varepsilon(Eu(OH)^{2+}, ClO_4^-)$	0.39 ± 0.04	Analogy with $Am(OH)^{2+}$ [31]
$\varepsilon(Eu(OH)_2^+, ClO_4^-)$	0.17 ± 0.04	Analogy with $Am(OH)_2^+$ [31]
$\varepsilon(Eu(CO_3)^+, ClO_4^-)$	0.17 ± 0.04	Analogy with $Am(CO_3)^+$ [31]
$\varepsilon(Eu(CO_3)_2^-, Na^+)$	−0.05 ± 0.05	Analogy with $Am(CO_3)_2^-$ [31]
$E(Eu(CO_3)_3^{3-}, Na^+)$	−0.23 ± 0.07	Analogy with $Am(CO_3)_3^{3-}$ [31]
$\varepsilon(EuAdip^+, ClO_4^-)$	0.10 ± 0.40	[29]

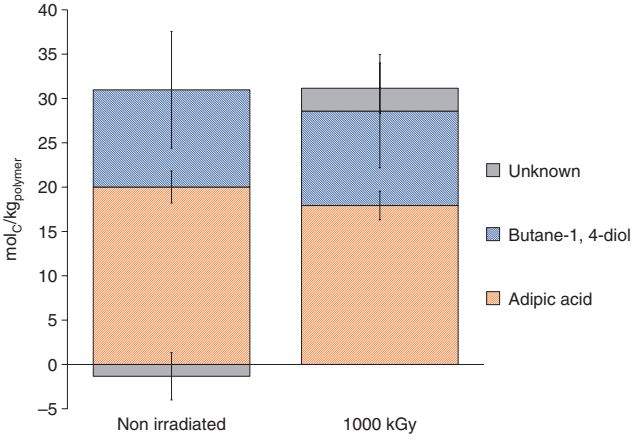

Figure 1: Mass balances on HDPs from non-irradiated PURe and γ-PURe, after leaching of PURe films in SACPW solution for one month at 60 °C. Error bars represent 2σ.

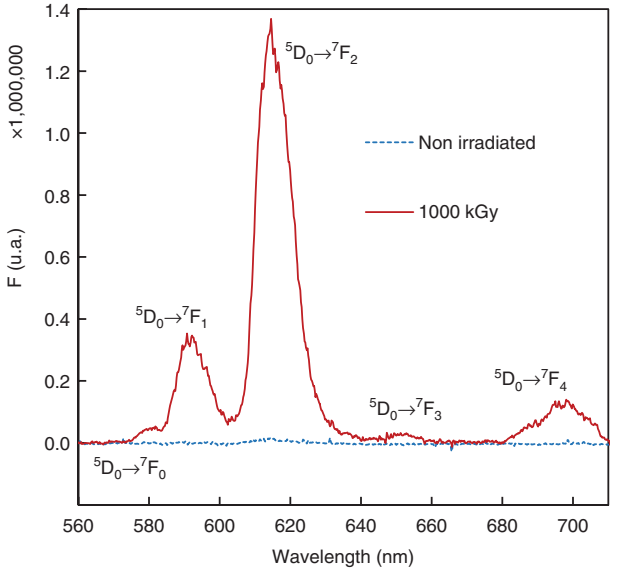

Figure 2: Luminescence spectra of Eu(III) in solution with HDPs from non-irradiated PURe (dotted line) and γ-PURe (plain line) in SACPW: [Eu] = 10^{-6} mol·kg$_w^{-1}$; D = 10 µs, W = 300 µs, λ_{exc} = 393.8 nm. HDPs are released after the leaching of the polymer in the SACPW solution for one month at 60 °C. HDPs were diluted by two to obtain these spectra.

conditions. This recalls $Cm(OH)_3(aq)$ in cement pore water [38]. The luminescence spectra of Eu(III) in the SACPW solution with representative amounts of BDO and adipic acid (Fig. S3b of the SI) is similar to the previous spectrum.

Figure 2 shows the Eu(III) luminescence spectra in HDPs solutions at pH 13.3. The spectrum obtained from the non-irradiated PURe-HDPs is equivalent to Eu(III), which suggests no interaction between Eu(III) and HDPs from the non-irradiated material. Conversely, the spectrum obtained with Eu(III) and the γ-PURe-HDPs show an important luminescence intensity. The $^5D_0 \rightarrow {}^7F_0$ transition – loss of centro-symmetry of Eu(III) complexes – is present, and the hypersensitive $^5D_0 \rightarrow {}^7F_2$ transition is more intense than the $^5D_0 \rightarrow {}^7F_1$ transition, evidencing the formation of Eu(III)-HDP complex(es).

The Eu(III) speciation under these conditions in the presence of adipic acid was calculated – Fig. S4 of the SI. The emission spectrum of Eu(III) in Fig. S3 of the SI shows that neither BDO nor adipic acid are responsible for the Eu(III) luminescence signal and complexation at pH 13.3. As a result, the ligands come from the unknown pool of HDPs shown on Figure 1. Even present in small proportion of the total amount of carbon, the complexing power seems important.

The excitation spectrum of Eu(III) complexed by the HDPs from the γ-PURe is compared to the one of Eu(III) at pH 4 in Figure 3. For free Eu(III) at pH 4, the luminescence signal is more important when the excitation wavelength is ca. 394 nm, which corresponds to the $^5L_6 \leftarrow {}^7F_0$ transition [30]. Before 392 nm and after 398 nm, the luminescence signal is very weak. The Eu(III) complexed by HDPs from γ-PURe shows a different excitation spectrum. Whatever the excitation wavelength from 390 to 400 nm, the intensity of the luminescence signal is almost constant. This so-called antenna effect – observed in literature in the case of aromatic ligands [17] – means that within the wavelength span the ligands are excited by the excitation wavelength and, after internal rearrangements, electrons are transferred to Eu(III) luminescent levels. The ligands energy levels must be located at least above the Eu(III) lowest luminescence levels ($\bar{\nu}$ = 17,277 cm^{-1} for $^5D_0 \rightarrow {}^7F_0$ and/or $\bar{\nu}$ = 19,028 cm^{-1} for $^5D_1 \rightarrow {}^7F_0$).

The luminescence of Eu(III) complexed by the γ-PURe HDPs is showing a bi-exponential decay (Fig. S8 of the SI), which can be attributed to the presence of two radiative decay processes from two different excited states. The first decay time $\tau_1 = 80 \pm 2$ µs (Table S4 of the SI) is faster than τ(Eu^{3+}), i. e. 110 µs [16], whereas the second decay time $\tau_2 = 340 \pm 8$ µs (Table S4 of the SI) is slower than τ(Eu^{3+}). This phenomenon was reported for the complexation of Eu(III) by humic substances [22–25] and in the case of Eu(III) complexed by HDPs from γ-irradiated PVC [5]. Complexed Eu(III) decay times faster than Eu^{3+} indicates inhibition mechanisms between Eu(III) and the ligands such as electrons transfers from Eu(III) excited states to the ligands [19, 39]. This particular behaviour was only observed with hydroxybenzoic ligands [19, 21, 39, 40]. The non-exponential luminescence decay also indicates the heterogeneity of the γ-PURe HDPs unknown pool.

In addition to UV-visible spectrum (Fig. S2 of the SI), antenna effect and bi-exponential luminescence decay indicate that the chemical structure of the ligands might be aromatic, which may seem sound considering that PURe is partly composed of aromatic segments (hard segments, Fig. S1 of the SI).

Following Fromentin and Reiller [29], the $^5D_0 \rightarrow {}^7F_2/{}^5D_0 \rightarrow {}^7F_1$ ratio ($^7F_2/{}^7F_1$) was investigated vs. C_{HDP} (Figure 4a) – the corresponding spectra are shown in Figure 4b normalized to the $^5D_0 \rightarrow {}^7F_1$ transition, and

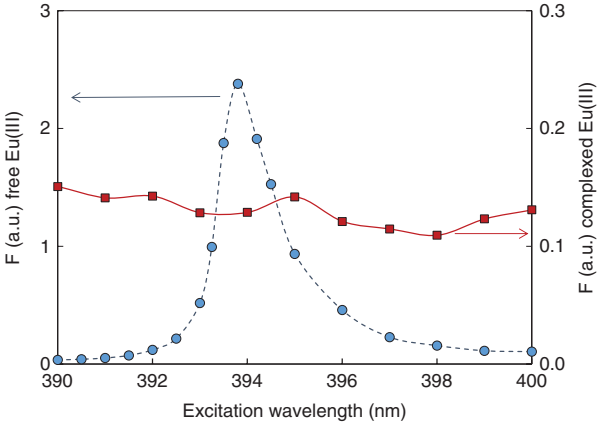

Figure 3: Excitation spectra of [Eu] = 10^{-6} mol·kg$_w^{-1}$ at pH 4.1 (blue circles, dashed line), and complexed by HDPs (1.6 mol·kg$_w^{-1}$) from γ-PURe in SACPW solution (red squares, solid line): D = 10 µs, *W* = 300 µs, 2000 accumulations.

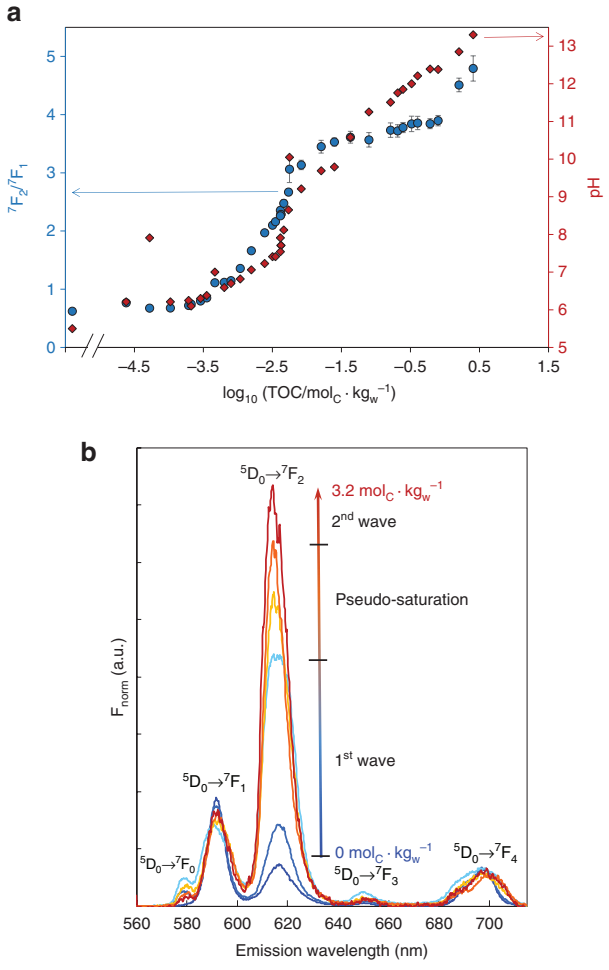

Figure 4: Eu(III) complexation isotherm of HDP (a) and luminescence spectra evolution (b).
Evolution of the $^7F_2/{}^7F_1$ ratio (circles) and pH (diamonds) in the presence of increasing C_{HDP} from γ-PURe on a logarithmic scale (a), evolution of the corresponding luminescence spectra of Eu(III) normalized to the area of the $^5D_0 \rightarrow {}^7F_1$ transition (b): [Eu] = 10^{-6} mol·kg$_w^{-1}$, D = 10 µs, W = 300 µs, λ_{exc} = 393.8 nm; error bars represent 2σ of the area ratio using the trapezoid method.

Fig. S5 of the SI normalized to the total area of the spectra. The nature of the ligands being unknown, the concentration was expressed vs. TOC. The ionic strength is not fixed either, because it is mainly controlled by the adipate ions concentration. However, the ionic strength was calculated for each solution considering that among HDPs only adipate ions influence the ionic strength. The evolution of $^7F_2/^7F_1$ with HDP dilution was also obtained at the pH value of the SACPW solution (Figure 5).

When C_{HDP} is nil, $^7F_2/^7F_1 = 0.62 \pm 0.02$. Then, $^7F_2/^7F_1$ increases with C_{HDP} until 3.6 ± 0.1 and being almost stable. This increase is called 'first wave' and the pseudo-steady state is called 'pseudo-saturation'. Then, while C_{HDP} reaches 1.6 $mol_C \cdot kg_w^{-1}$, $^7F_2/^7F_1$ increases again. This second increased will be named 'second wave' in the following. The presence of two waves indicates at least two Eu(III) complexes depending on C_{HDP}. As the pseudo-saturation zone shows a slight increase of $^7F_2/^7F_1$, one can infer that a third Eu(III)-HDP complex is existing. This is confirmed by the evolution at pH 13.3, which corroborates the increase in $^7F_2/^7F_1$. It must not be forgotten that as pH values are different, the implied complex(es) may not necessarily be the same even if $Eu(OH)_3(aq)$ should be major above pH 11.

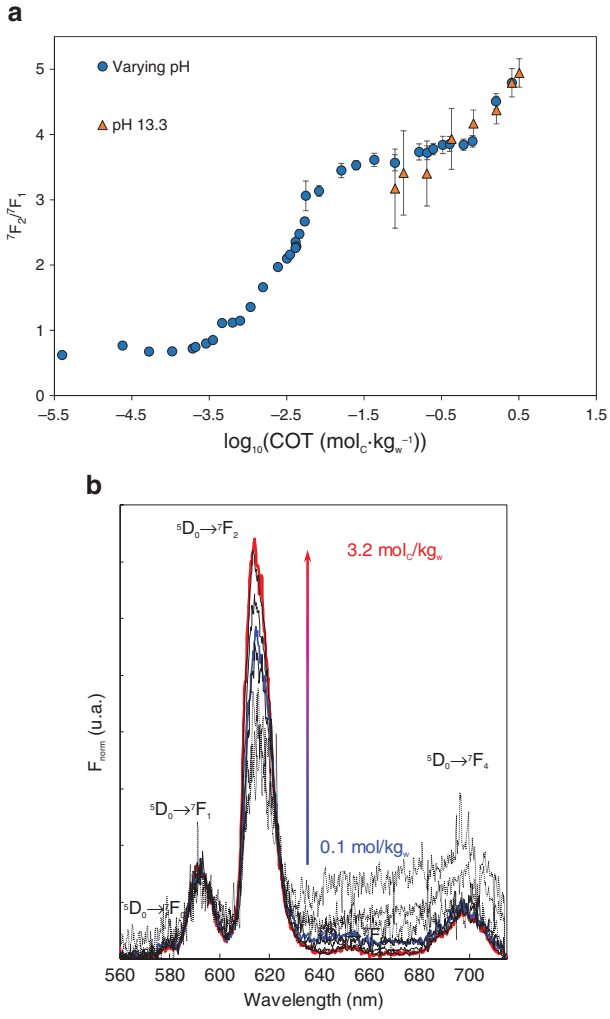

Figure 5: The evolution of $^7F_2/^7F_1$ with HDP dilution was also obtained at the pH value of the SACPW solution.
(a) Evolution of the $^7F_2/^7F_1$ ratio (circles) at varying pH from Figure 4, and at fixed pH 13.3 (triangles) in the presence of increasing C_{HDP} from γ-PURe on a logarithmic scale: $[Eu] = 10^{-6}$ $mol \cdot kg_w^{-1}$, D = 10 µs, W = 300 µs, $\lambda_{exc} = 393.8$ nm; error bars represent 2σ of the area ratio using the trapezoid method; (b) corresponding luminescence spectra at varying C_{HDP}.

The contribution of the $EuAdip^+$ complex in $^7F_2/^7F_1$ evolution vs. pH can be calculated from Fromentin and Reiller [29], which should represents less than 9.5 % (Fig. S9 of the SI) and is neglected in a first approximation. Moreover, we investigated the evolution of $^7F_2/^7F_1$ evolution of non-complexed Eu(III) vs. pH. In that case, $^7F_2/^7F_1$ does not exceed 2.5 (Fig. S10 of the SI). Hence, the $EuAdip^+$ and $Eu(OH)_n^{(3-n)+}$ species do not seem to be responsible for $^7F_2/^7F_1$ increase shown in Figure 4. Moreover, as already described elsewhere, the $Eu(CO_3)_3^{(3-2n)+}$ complexes are not suspected [5].

The luminescence spectra presented in Figure 4b and Fig. S7 of the SI also shows that $^5D_0 \rightarrow {}^7F_0$ transition intensity increases up to the pseudo-saturation state, then strongly decreases. This is indicating that the Eu(III) chemical environment corresponding to the second wave is more centro-symmetric than the one of the first wave. The same observation was made in the case of Eu(III) complexed by HDPs from γ-irradiated PVC [5]. A slight modification of the shape of the $^5D_0 \rightarrow {}^7F_1$ transition is also noticed, which was already observed for Eu-humic acid complexes [24]. This transition is less sensitive to the chemical environment, but indicates a modification of the crystal field stabilization of energy, which confirms the symmetry changes indicated by the $^5D_0 \rightarrow {}^7F_0$ transition evolution [20]. Finally, a modification of the $^5D_0 \rightarrow {}^7F_4$ transition is also apparent in Figure 4b – more clearly in Fig. S5 of the SI. In view of its high multiplicity, interpretation of the modification of this band is not straightforward [20].

3.3.2 Study of the complexes

In the following sections, we will first focus on the first wave part of the Figure 4, corresponding to $6 \leq pH \leq 10$ and C_{HDP} up to 0.08 $mol_C \cdot kg_w^{-1}$. A pseudo-saturation state is obtained, which allows estimating the complexing power of HDPs in this area. Then we will focus on the second part of the isotherm at varying C_{HDP} and $pH \geq 10$, and on the constant pH 13.3. Finally, an identification of complexing molecules will be undertaken.

3.3.2.1 Quantification of the complexation power of HDPs for pH 6–10

The formation constants can only be global without the knowledge of HDPs' functionality. Considering the simple equilibrium between non-complexed europium (Eu_{nc}) and a carbon originated from the HDP (HDP_C), one can write the following operational equilibrium with associated operational constant K_{op}.

$$Eu_{nc} + mHDP_C = Eu(HDP_C)_m$$

$$K_{op} = K_{op} = \frac{\left[Eu(HDP_c)_m\right]}{\left[Eu_{nc}\right]\left[HDP_c\right]^m} \quad (1)$$

The mass balance on Eu_{nc} is written as follows.

$$[Eu_{nc}] = [Eu^{3+}] + [Eu(OH)^{2+}] + [Eu(OH)_2^{+}] + [Eu(OH)_3(aq)] + [EuAdip^{+}]$$

The plot of $\log_{10}([Eu(HDP_C)_m]/[Eu_{nc}])$ vs. $\log_{10}[HDP_C]$ in Figure 6a is showing a slope close to unity (Table 3) and $\log_{10}K_{op,Eu} = 3.9_3 \pm 0.1_4$ (1σ) at the intercept. Note that from $\log_{10}[HDP_C] = -2.3$ the data seem not to be linear.

This operational constant can also be plotted against the free ion Eu^{3+} concentration, considering the hydrolysis constants of Eu(III) (Tables 1 and 2) and the formation constant of the $EuAdip^{+}$ complex [29] as follows.

$$[Eu_{nc}] = [Eu^{3+}] \times \left(1 + \sum \frac{{}^*\beta_n}{[H^+]^n}\right) = [Eu^{3+}]\alpha_{Eu^{3+}} \quad (2)$$

The plot of $\log_{10}([Eu(HDP_C)_m]/[Eu^{3+}])$ vs. $\log_{10}[C_{HDP}]$ in Figure 6b is evidencing two zones. The first one is described by a straight line ($r^2 = 0.9828$) and corresponds to a 1:1 stoichiometry and $\log_{10}K_{op} = 4.28 \pm 0.16$ (1σ). The second area is less linear and gives a higher stoichiometry,

$$Eu^{3+} + 8HDP_C = Eu(HDP_C)_8$$

with a higher $\log_{10}K_{op} = 22.0 \pm 4.3$ (1σ).

As already stressed [5], the variation here is dual: the HDPs are diluted with no pH adjustment, meaning that the variation is both due to pH and C_{HDP}. But the pH variation cannot be firmly attributed to an eventual acidity of the HDPs – other than the already ionized adipic acid under these conditions – or to the hydrolysis of Eu(III). As we do not have any information upon the functionality of HDPs – quantity of complexation sites or eventual pK_a –, the slope analyses can only be done considering the $Eu(OH)_n^{(3-n)+}$ complexes. The slopes, $\log_{10}K_{op}$, and determination coefficients are reported in Table 3. Some analyses indicate negative – or close to zero – slopes, meaning that no complexation occurs with the considered non-complexed Eu(III) species or that a lower hydroxo complex should be considered. Whatever the considered non-complexed Eu(III) species, a change of slope is always occurring at $[HDP_C] = 3.5\ 10^{-3}\ mol_C \cdot kg_w^{-1}$. First slope is always either close to unity or close to zero. In this area, there may be a short chained HDP composed of one carbon which is complexing Eu(III). The only complexing organic molecule with one carbon are carbonate and formate. Formate is not detected in a sufficient amount to be responsible of the complexation phenomenon. The formation of the $Eu(CO_3)^{+}$ may be possible but its luminescence signal is presenting a higher ${}^5D_0 \rightarrow {}^7F_0$ transition than it is observed here [41, 42]. Another possibility is that the TOC analyses are biased and do not represent the total amount of dissolved carbon. We have up to now no argument in favour of either hypotheses.

As we have demonstrated before, ${}^7F_2/{}^7F_1$ of the hydroxo Eu(III) species can reach 2.5. As a result, below this value, which corresponds to the area we are discussing, the contribution cannot be neglected. Consequently, this slope may also be induced by the non-complexed Eu(III) species. However, it is sure that the non-complexed Eu(III) species do not contribute to the second slope. The second slope always indicates a higher stoichiometry, which is more likely to correspond to one HDP or a group of several HDPs. The associated constant is also always relatively high.

The same behaviour was observed for the complexation of Eu(III) by HDPs from a radio-oxidized PVC [5]. This is somewhat surprising because the chemical formulations of PURe and PVC are very different, so the degradation mechanisms and the resulting HDPs are thought to be different. This commonality may be a coincidence or the indication of some commonalities that are not understood, yet.

3.3.2.2 Complexation at pH above 10

Appreciating the complexation of the second wave at various pH is not straightforward, as the final plateau is not attained. Figure S6 of the SI shows the evolution of ${}^7F_2/{}^7F_1$ on the direct scale evidencing that a plateau is almost attained for data at constant pH 13.3. More data should be obtained but it was not possible due to the limited amount of sample. The same treatment than in previous section was applied at pH 13.3 in Figure 5 yielding to the plot in Figure 7a. The slope of 1.3 ± 0.1 suggest a stoichiometry close to one between Eu^{3+} and the HDPs on the mole of carbon basis, and $\log_{10}K = 15.9 \pm 0.7$ (2σ) is obtained.

One can remember that the proposed value for HDPs from radio-oxidized PVC did not satisfactorily fit

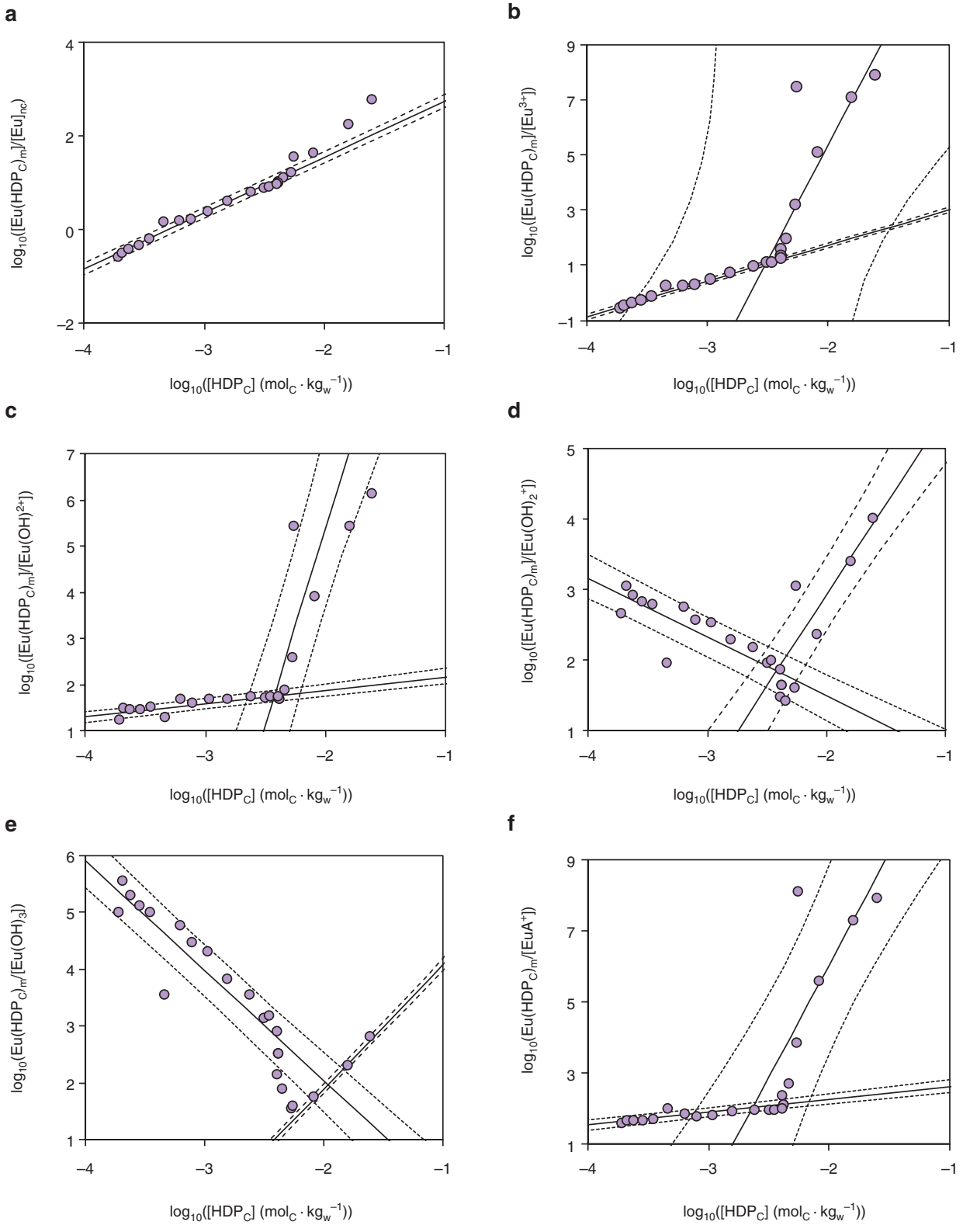

Figure 6: Slope analyses of the Eu(III)-HDP complexation isotherms at varying C_{HDP}.
Determination of the Eu(III)-HDP complexes stoichiometries and $\log_{10}K_{op}$ from TRLS results from Figure 4 considering (a) total non-complexed europium, (b) Eu^{3+} free, (c) $Eu(OH)^{2+}$, (d) $Eu(OH)_2^+$, (e) $Eu(OH)_3$(aq), and (f) $EuAdip^+$ in solution using hydrolysis constant (Table 1) corrected using SIT parameters (Table 2). $[Eu] = 10^{-6}$ mol·kg_w^{-1}. The solid lines correspond to the linear regressions whereas the dashed lines correspond to the uncertainties (1σ).

Table 3: Possible slope analyses of Figures 6 and 7.

Equilibrium	Slope	r^2	$Log_{10}k_{op}$
$Eu_{nc} + HDP = EuHDP$	1.19 ± 0.05	0.9731	3.93 ± 0.14
$Eu^{3+} + HDP = EuHDP$	1.29 ± 0.05	0.9828	4.28 ± 0.16
$Eu3+ + 8HDP = Eu(HDP)_8$	8.3 ± 2.0	0.6914	22.0 ± 4.3
$Eu(OH)^{2+} + 6HDP = Eu(OH)(HDP)_6$	5.5 ± 1.3	0.7233	15.4 ± 2.8
$Eu^{3+} + H_2O + 6HDP = Eu(OH)(HDP)_6 + H+$			−2.1 ± 2.8
$Eu(OH)_2^{+} + 3HDP = Eu(OH)_2(HDP)_3$	2.6 ± 0.6	0.8061	8.1 ± 1.3
$Eu^{3+} + 2H_2O + 3HDP = Eu(OH)_2(HDP)_3 + 2H+$			−7.0 ± 1.3
$Eu(OH)_3(aq) + 2HDP = Eu(OH)_3(HDP)_2$	2.2 ± 0.2	0.9919	6.3 ± 0.4
$Eu^{3+} + 3H_2O + 2HDP = Eu(OH)_3(HDP_2 + 3H^+$			−18.1 ± 0.9
pH = 13.3			
$Eu3+ + HDP = Eu(HDP)$	1.3 ± 0.1	0.9748	15.9 ± 0.1
$Eu(OH)_2+ + HDP = Eu(OH)_2(HDP)$	1.3 ± 0.1	0.9748	5.1 ± 0.2
$Eu3+ + 2H_2O + HDP = Eu(OH)_2(HDP)$			−10.7 ± 0.4

Charge of the complexes are omitted because of the lack of knowledge on the functionality of HDPs.

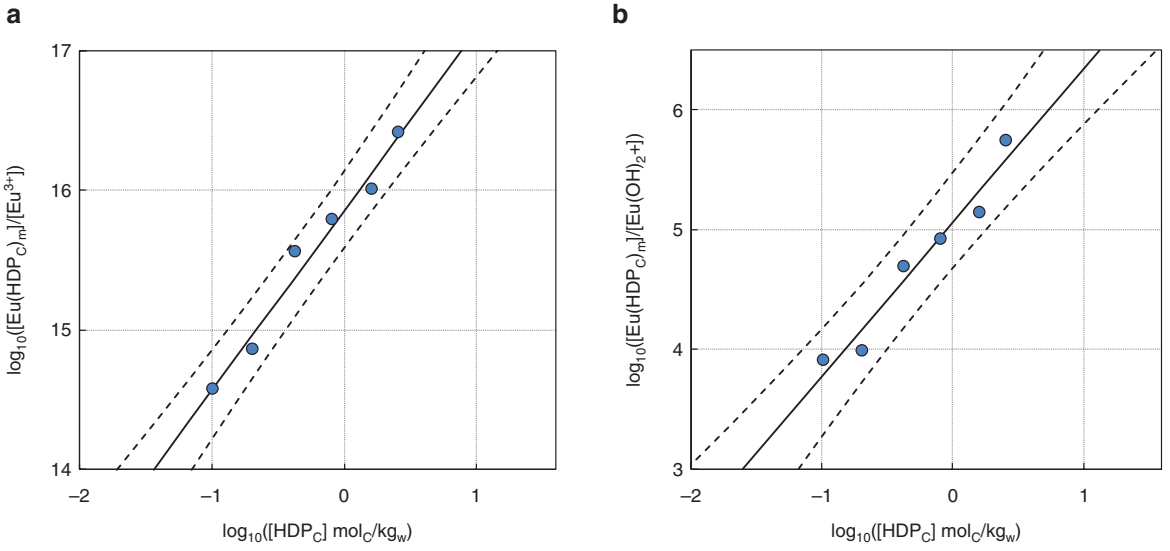

Figure 7: Slope analyses of the complexation isotherm at constant pH.
Determination of the Eu(III)-HDP complexes stoichiometries and $log_{10}K_{op}$ from TRLS results from Figure 4 at pH = 13.3 considering (a) Eu^{3+} free, and (b) $Eu(OH)_2^{+}$ in solution using hydrolysis constants (Table 1) corrected using SIT parameters (Table 2). [Eu] = 10^{-6} mol·kg_w^{-1}. The solid lines correspond to the linear regressions whereas the dashed lines correspond to the uncertainties (1σ).

the solubility data and the formation of $Eu(OH)_2HDP$ seemed to be more adequate [5]. The account of the formation of $Eu(OH)_2HDP$ yield also to a 1.3 ± 0.15 slope and a $log_{10}K_{op} = 5.06 \pm 0.16$ (2σ) (Figure 7b). When considering the following equilibrium.

$$Eu^{3+} + 2H_2O + HDP \rightleftarrows Eu(OH)_2HDP$$

Then the operational constant becomes $log_{10}K_{op} = -10.7 \pm 0.2$.

These values are difficult to compare directly with the case of PVC as different stoichiometries are obtained. Nevertheless, it seems that a significant amount of europium(III), can be complexed by the γ-PURe-HDPs. The extent to which this complexation can induce a mobilization of radionuclide from a nuclear wastes disposal will depend on the adsorption of the HDPs and complexed metals onto cementitious phases [43]. A comparison between the two cases will be presented afterward.

3.3.2.3 Identification of some ligands

The identification of the HDPs ligands in the 6 ≤ pH ≤ 10 area was attempted by ESI-MS-MS. The direct characterization

of ligands above pH 10 area cannot be achieved due to high Na^+ and K^+ concentrations used to reach such pH values. Natural Eu isotopic pattern is easily noticeable among the HDPs isotopic pattern [44] (Fig. S11 of the SI). Figure 8 shows the ESI-MS spectrum of Eu in solution with HDPs at pH 9.4. The spectrum shows signals which corresponds to non-complexed Eu – i. e. ions at m/z 167.9–169.9 and 221.9–223.9 –, and to Eu complexed by adipate. Thanks to ESI-MS-MS analyses (Fig. S12 of the SI), these signals were attributed in Table 4 to Eu complexed by adipic acid – i. e. ions at m/z 269.0–298.0 and 314.0–316.0 – and to adipate with salt adducts (KOH and NaOH) – i. e. ions m/z 706.9–708.9 and 722.9–724.9 –. Additionally, Eu complexed by soft segment oligomer (LH_2) was also identified. The chemical structure is reported in Figure 8, and corresponding signals can be observed at ions m/z 385.0–387.0 and 403.0–405.0. It was already shown that adipate is complexing Eu(III) below pH 10. One can note that adipate and the oligomer cannot be responsible for the antenna effect observed at pH 13.3 (cf. Figure 3), which confirms the different chemical structure of the ligands at $6 \leq pH \leq 10$ (first wave) and at $pH > 10$ (second wave).

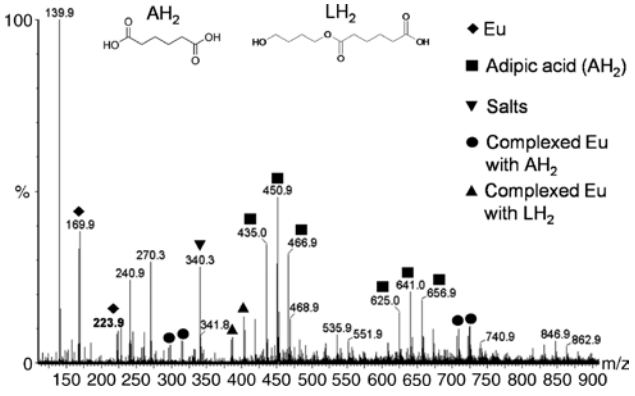

Figure 8: ESI-MS spectrum in positive mode of Eu in solution with HDPs from γ-PURe: $[Eu] = 10^{-6}$ $mol \cdot kg_w^{-1}$, pH = 9.4; HDPs are released after the leaching of the polymer in ASCPW solution for one month at 60 °C. The signal attributions in Table 4 were done by ESI-MS-MS, and correspond to Eu complexed by adipic acid (AH_2) and a soft segment oligomer (LH_2).

Table 4: Attribution of signals of Figure 8 that present the Eu isotopic pattern.

Peaks (m/z)	Attribution
167.9–169.9	$[Eu(OH)]^+$
221.9–223.9	$[Eu(OH)(H_2O)_3]^+$
260.0–262.0	Not attributed
269.0–298.0	$[Eu(AdipH)]^+$
314.0–316.0	$[Eu(AdipH)(H_2O)]^+$
385.0–387.0	$[Eu(L)(H_2O)]^+$
403.0–405.0	$[Eu(L)(H_2O)_2]^+$
706.9–708.9	$[Eu(Adip)_3(K)_2(Na)_2]^+$
722.9–724.9	$[Eu(Adip)_3(K)_2(Na)_2(H_2O)]^+$

AH_2, adipic acid; LH_2, soft segment oligomer.

3.4 Implication on the luminescence properties of Eu(III) in γ-PURe-HDP

One can remind that bi-exponential decays have been evidenced both in γ-PURe-HDP (Fig. S8 of the SI) but also in γ-PVC-HDPs [5]. The occurrence of non-exponential decays is linked to two different excitation states, which exchange is slow enough to be evidenced by the technique. It can come either from two different species or from two different excited states. In this work, we have evidenced three different possible species in a wide range of pH values. The bi-exponential decays in Fig. S8 of the SI were determined in only one condition and cannot represent the different possible species evidenced. It explains why a third decay time was not evidenced in Fig. S8 of the SI. Furthermore, it seems difficult to affect a species to a particular decay time. It seems that the occurrence of the bi-exponential decay is mainly linked the composition of the HDPs and not to the particular complexing entities or complexes formed.

3.5 Implication on Eu(III) solubility and speciation in the pH/C(γ-PURe-HDP) studied domain

In order to compare these results on HDPs from 1000 kGy γ-PURe to our previous results on 10 MGy γ-PVC, the solubility surfaces of $Eu(OH)_3(am)$ and $EuOHCO_3(cr)$ are calculated using thermodynamic constants in Table 1 – and specific interaction parameters in Table 2 – and operational constants for EuHDP and $Eu(OH)_3HDP_2$ in Table 3. Calculation were done using PhreeqCI 3.4.0.1297 software [45, 46], using the hydrolysed forms of the operational constants and impeding the modification of the operational constants with ionic strength.

The solubility enhancement of $0.01\ mol \cdot kg_w^{-1}$ $Eu(OH)_3(am)$ by γ-PURe HDPs – on carbon basis – as a function of pH is shown in Figure 9a. It can be seen that the influence of the HDPs is more important for the HDPs from the 1000 kGy γ-PURe compared to the 10 MGy γ-PVC estimated in Reiller et al. [5]. An amount of ca. 10^{-2} $mol_C \cdot kg_w^{-1}$ of γ-PURe-HDPs is necessary to increase the $Eu(OH)_3(am)$ solubility by two orders of magnitude in an alkaline solution, where more than 1 $mol_C \cdot kg_w^{-1}$ were necessary for the

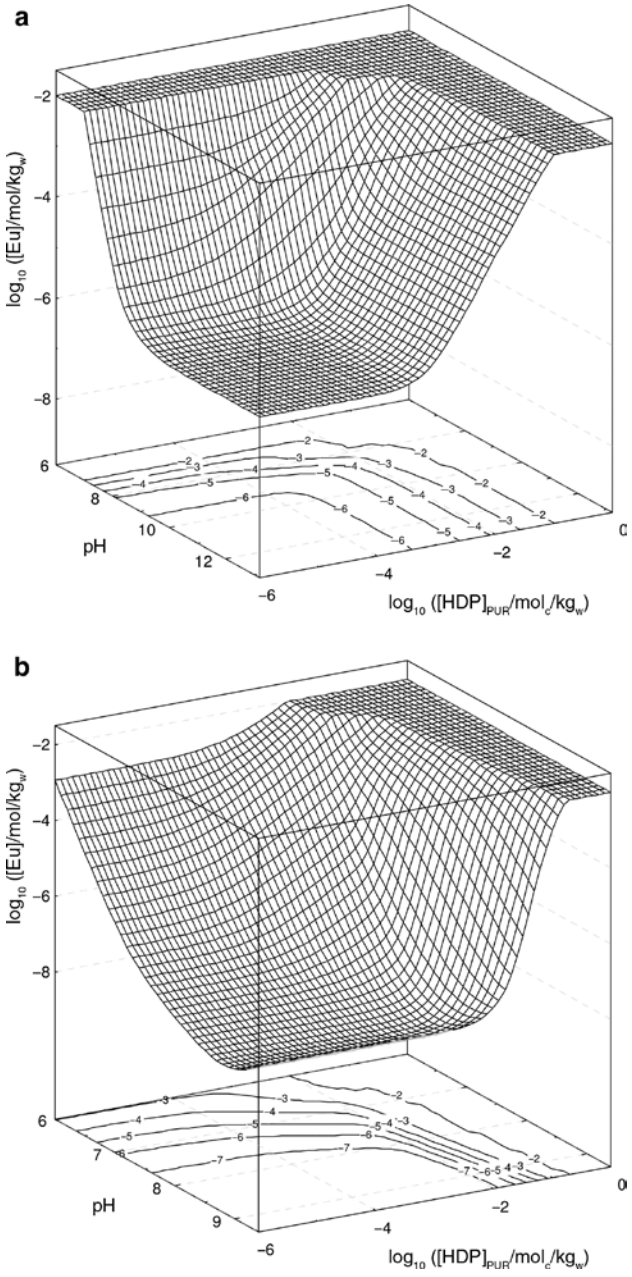

Figure 9: The solubility enhancement of 10.01 mol·kg$_w^{-1}$ Eu(OH)$_3$(am) by γ-PURe HDP and comparison with the solubility of EuOHCO$_3$(cr) at atmospheric CO$_2$(g) pressure.
Solubility of $[Eu]_{total} = 0.01$ mol·kg$_w^{-1}$ as a function of pH and concentration of 1000 kGy γ-PURe-HDP (on total carbon basis) using thermodynamic constants (Tables 1, and 2) and formation constants for EuHDP and Eu(OH)$_3$HDP$_2$ in Table 3 of (a) Eu(OH)$_3$(am) at $PCO_2(g) = 10^{-12}$ atm, and (b) EuOHCO$_3$(cr) at $PCO_2(g) = 10^{-3.5}$ atm.

γ-PVC-HDPs. It can also be seen that the complexation is also extending down to mildly alkaline pH region in a wider parametric space comparing to γ-PVC-HDPs.

The comparison with the solubility of EuOHCO$_3$(cr) at atmospheric CO$_2$(g) pressure is shown in Figure 9b. It can also be seen that the solubility domain of Eu is enhanced by the γ-PURe HDPs. At pH 9.5, a concentration of ca. 0.1 mol$_C$·kg$_w^{-1}$ of 1000 kGy γ-PURe is necessary to increase the solubility of EuOHCO$_3$(cr) by two orders of magnitude, when ca. 1 mol·kg$_w^{-1}$ was necessary for 10 MGy γ-PVC-HDPs. The extent of complexation is also more important in more neutral medium, and extends down to ca. 10^{-3} mol$_C$·kg$_w^{-1}$.

It seems that the complexing power of the γ-PURe-HDPs is more important than the one of γ-PVC-HDPs. Nevertheless, we are still lacking of the sufficient amount of knowledge on the functionality of the HDPs, and the comparison between doses is not possible. A particular effort of the evaluation of the functionality seems desirable.

4 Conclusions

Our aim was to investigate the complexation of Eu(III) by HDPs leached from a non-formulated PURe irradiated with γ-rays in an ASCPW solution (pH 13.3). Unlike HDPs from non-irradiated PURe, the γ-PURe-HDPs can complex Eu(III) in alkaline media. It was shown that neither adipic acid nor butane-1,4-diol, the two main HDPs, were responsible for this complexation under these conditions. The UV-Visible spectrum of the HDPs, and an antenna effect and a bi-exponential luminescence decay of complexed Eu(III) in TRLFS seem to indicate that the ligands, or ligand pools, are likely to contain aromatic structures.

The existence of two to three complex states was evidenced. The complexes formed at high pH (from 10 to 13) are different from the lower pH complexes. Complexation reactions and operational constants were proposed. Two ligands in the lower pH range were identified: adipic acid and an oligomer issued from the soft segments of PURe.

By comparison to γ-PVC, it seems that the complexation power of γ-PURe is more important as it lowers the necessary amount to dissolve Eu(OH)$_3$(am) by two orders of magnitude in a highly alkaline medium, and one order of magnitude for EuOHCO$_3$(cr).

In an industrial context, HDPs may be able to complex lanthanides/actinides(III) in cemented waste packages, but also in more neutral conditions such as in argillaceous host rocks. Attention have to be paid to the effect of HDPs and induced complexations on the radionuclides mobility and adsorption to the disposal engineered barriers.

Acknowledgements: The authors acknowledge ORANO and EDF for financial support and fruitful discussions;

Sophie Rouif (IONISOS); Emmanuel Buiret (FILAB); Annick Geysen and Julie Goldberg (Lubrizol); and Solène Legand, Cyrielle Jardin and Jean-Luc Roujou (CEA).

References

1. Lamouroux, C., Cochin, F.: Study of long term behavior of intermediate level long lived waste packages: An overview of the R&D approach and results. Procedia Chem. **7**, 559 (2012).
2. Keith-Roach, M. J.: The speciation, stability, solubility and biodegradation of organic co-contaminant radionuclide complexes: a review. Sci. Total Environ. **396**, 1 (2008).
3. Van Loon, L. R., Hummel, W.: The degradation of strong basic anion exchange resins and mixed-bed ion-exchange resins: effect of degradation products on radionuclide speciation. Nucl. Technol. **128**, 388 (1999).
4. Dannoux, A.: Extrapolation dans le Temps des Cinétiques de Production des Produits de Dégradation Radiolytique: Application à un Polyuréthane, PhD, Université Paris XI, Orsay, France (2007).
5. Reiller, P. E., Fromentin, E., Ferry, M., Dannoux-Papin, A., Badji, H., Tabarant, M., Vercouter, T.: Complexing power of hydro-soluble degradation products from γ-irradiated polyvinylchloride: influence on $Eu(OH)_3(s)$ solubility and Eu(III) speciation in neutral to alkaline environment. Radiochim. Acta **105**, 665 (2017).
6. Baston, G. M. N., Cowper, M., Davies, P., Dawson, J., Farahani, B., Heath, T., Schofield, J., Smith, V., Watson, S., Wilson, J.: The Impact of PVC Additives and their Degradation Products on Radionuclide Behaviour, Amec Foster Wheeler, Report FW/0006604/4, Harwell, Oxford, UK (2017).
7. ANDRA: Évaluation de la faisabilité d'un stockage géologique en formation argileuse. Dossier 2005 Argile, Chatenay Malabry, France (2005), p. 239.
8. Berner, U. R.: Evolution of pore water chemistry during degradation of cement in a radioactive waste repository environment. Waste Manage. **12**, 201 (1992).
9. Nixon, S. L., van Dongen, B. E., Boothman, C., Small, J. S., Lloyd, J. R.: Additives in plasticised polyvinyl chloride fuel microbial nitrate reduction at high pH: Implications for nuclear waste disposal. Front. Environ. Sci. **6**, 97 (2018).
10. Baston, G. M. N., Berry, J. A., Bond, K. A., Boult, K. A., Brownsword, M., Linklater, C. M.: Effects of cellulosic degradation products on uranium sorption in the geosphere. J. Alloys Compd. **213**, 475 (1994).
11. Van Loon, L. R., Glaus, M. A.: Review of the kinetics of alkaline degradation of cellulose in view of its relevance for safety assessment of radioactive waste repositories. J. Environ. Polym. Degr. **5**, 97 (1997).
12. Glaus, M. A., Van Loon, L. R.: Degradation of cellulose under alkaline conditions: new insights from a 12 years degradation study. Environ. Sci. Technol. **42**, 2906 (2008).
13. Diesen, V., Forsberg, K., Jonsson, M.: Effects of cellulose degradation products on the mobility of Eu(III) in repositories for low and intermediate level radioactive waste. J. Hazard. Mater. **340**, 384 (2017).
14. Van Loon, L. R., Hummel, W.: Radiolytic and chemical degradation of strong acidic ion-exchange resins: Study of the ligands formed. Nucl. Technol. **128**, 359 (1999).
15. Pearson, R. G.: Hard and soft acids and bases. J. Am. Chem. Soc. **85**, 3533 (1963).
16. Horrocks Jr., W. D., Sudnick, D. R.: Lanthanide ion probes of structure in biology. Laser-induced luminescence decay constants provide a direct measure of the number of metal-coordinated water molecules. J. Am. Chem. Soc. **101**, 334 (1979).
17. Alpha, B., Ballardini, R., Balzani, V., Lehn, J.-M., Perathoner, S., Sabbatini, N.: Antenna effect in luminescent lanthanide cryptates: a photophysical study. Photochem. Photobiol. **52**, 299 (1990).
18. Wang, Z. M., van de Burgt, L. J., Choppin, G. R.: Spectroscopic study of lanthanide(III) complexes with aliphatic dicarboxylic acids. Inorg. Chim. Acta **310**, 248 (2000).
19. Kuke, S., Marmodée, B., Eidner, S., Schilde, U., Kumke, M. U.: Intramolecular deactivation processes in complexes of salicylic acid or glycolic acid with Eu(III). Spectrochim. Acta A **75**, 1333 (2010).
20. Binnemans, K.: Interpretation of europium(III) spectra. Coord. Chem. Rev. **295**, 1 (2015).
21. Burek, K., Eidner, S., Kuke, S., Kumke, M. U.: Intramolecular deactivation processes of electronically excited lanthanide(III) complexes with organic acids of low molecular weight. Spectrochim. Acta A **191**, 36 (2017).
22. Brevet, J., Claret, F., Reiller, P. E.: Spectral and temporal luminescent properties of Eu(III) in humic substance solutions from different origins. Spectrochim. Acta A **74**, 446 (2009).
23. Reiller, P. E., Brevet, J.: Bi-exponential decay of Eu(III) complexed by Suwannee River humic substances: spectroscopic evidence of two different excited species. Spectrochim. Acta A **75**, 629 (2010).
24. Janot, N., Benedetti, M. F., Reiller, P. E.: Influence of solution parameters on europium(III), α-Al_2O_3, and humic acid interactions: macroscopic and time-resolved laser-induced luminescence data. Geochim. Cosmochim. Acta **123**, 35 (2013).
25. Kouhail, Y. Z., Benedetti, M. F., Reiller, P. E.: Eu(III)–fulvic acid complexation: evidence of fulvic acid concentration dependent interactions by time-resolved luminescence spectroscopy. Environ. Sci. Technol. **50**, 3706 (2016).
26. Moreau, P., Colette-Maatouk, S., Gareil, P., Reiller, P. E.: Influence of hydroxybenzoic acids on the adsorption of Eu(III) onto α,γ-Al_2O_3 particles in mildly acidic conditions: a macroscopic and spectroscopic study. Appl. Geochem. **74**, 13 (2016).
27. Fromentin, E., Aymes-Chodur, C., Doizi, D., Cornaton, M., Miserque, F., Cochin, F., Ferry, M.: On the radio-oxidation, at high doses, of an industrial polyesterurethane and its pure resin. Polym. Degrad. Stab. **146**, 161 (2017).
28. Fromentin, E., Pielawski, M., Lebeau, D., Esnouf, S., Cochin, F., Legand, S., Ferry, M.: Leaching of radio-oxidized poly(ester urethane): Water-soluble molecules characterization. Polym. Degrad. Stab. **128**, 172 (2016).
29. Fromentin, E., Reiller, P. E.: Influence of adipic acid on the speciation of Eu(III): Review of thermodynamic data in NaCl and $NaClO_4$ media, and a new determination of Eu-adipate complexation constant in 0.5 $mol.kg_w^{-1}$ $NaClO_4$ medium by time-resolved luminescence spectroscopy. Inorg. Chim. Acta **482**, 588 (2018).
30. Carnall, W. T., Fields, P. R., Rajnak, K.: Electronic energy levels of trivalent lanthanide aquo ions. IV. Eu^{3+}. J. Chem. Phys. **49**, 4450 (1968).
31. Guillaumont, R., Fanghänel, T., Neck, V., Fuger, J., Palmer, D. A., Grenthe, I., Rand, M. H.: Update on the Chemical Thermo-

dynamics of Uranium, Neptunium, Plutonium, Americium and Technetium, OECD Nuclear Energy Agency, Issy-les-Moulineaux, France (2003), p. 918.
32. Hummel, W., Berner, U. R., Curti, E., Pearson, F. J., Thoenen, T.: Nagra/PSI Chemical Thermodynamic Data Base 01/01, NAGRA, Report NTB 02-06, Wettingen, Switzerland (2002), p. 564.
33. Rao, R. R., Chatt, A.: Studies on stability constants of europium(III) carbonate complexes and application of SIT and ion-pairing models. Radiochim. Acta **54**, 181 (1991).
34. Vercouter, T., Vitorge, P., Trigoulet, N., Giffaut, E., Moulin, C.: $Eu(CO_3)_3^{3-}$ and the limiting carbonate complexes of other M^{3+} f-elements in aqueous solutions: a solubility and TRLFS study. New J. Chem. **29**, 544 (2005).
35. Korshin, G. V., Li, C.-W., Benjamin, M. M.: Monitoring the properties of natural organic matter through UV spectroscopy: a consistent theory. Water Res. **31**, 1787 (1997).
36. Claret, F., Schäfer, T., Brevet, J., Reiller, P. E.: Fractionation of Suwannee River fulvic acid and Aldrich humic acid on α-Al_2O_3: spectroscopic evidence. Environ. Sci. Technol. **42**, 8809 (2008).
37. Del Vecchio, R., Blough, N. V.: On the origin of the optical properties of humic substances. Environ. Sci. Technol. **38**, 3885 (2004).
38. Tits, J., Stumpf, T., Rabung, T., Wieland, E., Fanghänel, T.: Uptake of Cm(III) and Eu(III) by calcium silicate hydrates: a solution chemistry and time-resolved laser fluorescence spectroscopy study. Environ. Sci. Technol. **37**, 3568 (2003).
39. Primus, P.-A., Kumke, M. U.: Flash photolysis study of complexes between salicylic acid and lanthanide ions in water. J. Phys. Chem. A **116**, 1176 (2012).
40. Moreau, P., Colette-Maatouk, S., Vitorge, P., Gareil, P., Reiller, P. E.: Complexation of europium(III) by hydroxybenzoic acids: a time-resolved luminescence spectroscopy study. Inorg. Chim. Acta **432**, 81 (2015).
41. Vercouter, T.: Complexes Aqueux de Lanthanides (III) et Actinides (III) avec les Ions Carbonates et Sulfates. Etude Thermodynamique par Spectrofluorimétrie Laser Résolue en Temps et Spectrométrie de Masse à Ionisation Électrospray, Université Evry-Val d'Essonne, Evry, France (2005), p. 253.
42. Kouhail, Y. Z.: Influence de la Compétition des Anions (Hydroxyde, Carbonate) sur la Complexation des Lanthanides Trivalents par la Matière Organique Naturelle: Cas des Substances Humiques, Université Paris Diderot, Paris, France (2016).
43. von Schenck, H., Källström, K.: Reactive transport modelling of organic complexing agents in cement stabilized low and intermediate level waste. Phys. Chem. Earth Pt A/B/C **70–71**, 114 (2014).
44. Meija, J., Coplen, T. B., Berglund, M., Brand, W. A., de Bièvre, P., Gröning, M., Holden, N. E., Irrgeher, J., Loss, R. D., Walczyk, T., Prohaska, T.: Isotopic compositions of the elements 2013 (IUPAC Technical Report). Pure Appl. Chem. **88**, 293 (2016).
45. Parkhurst, D. L., Appelo, C. A. J.: User's Guide to PHREEQC (Version 2) – A Computer Program for Speciation, Batch-Reaction, One-Dimensional Transport, and Inverse Geochemical Calculations, U.S. Geological Survey, Water-Resources Investigations, Report 99-4259, Lakewood, Colorado, USA (1999).
46. Parkhurst, D. L., Appelo, C. A. J.: Description of Input and Examples for PHREEQC Version 3 – A Computer Program for Speciation, Batch-Reaction, One-Dimensional Transport, and Inverse Geochemical Calculations. Chapter 43 of Section A, Groundwater Book 6, Modeling Techniques, U.S. Geological Survey, Denver, Colorado, USA (2013), p. 497.

Supplementary Material: The online version of this article offers supplementary material (https://doi.org/10.1515/ract-2019-3122).